Thermally induced atomic diffusion at the interface between release agent coating and mould substrate in a glass moulding press

2011 J. Phys. D: Appl. Phys. 44 215302

(http://iopscience.iop.org/0022-3727/44/21/215302)

IOP PUBLISHING JOURNAL OF PHYSICS D: APPLIED PHYSICS

J. Phys. D: Appl. Phys. **44** (2011) 215302 (12pp) doi:10.1088/0022-3727/44/21/215302

Thermally induced atomic diffusion at the interface between release agent coating and mould substrate in a glass moulding press

Jun Masuda[1], Jiwang Yan[2], Tianfeng Zhou[2], Tsunemoto Kuriyagawa[2] and Yasushi Fukase[1]

[1] Toshiba Machine Co., Ltd, Ooka 2068-3, Numazu-Shi, Shizuoka-Ken, 410-8510, Japan
[2] Department of Mechanical Systems and Design, Graduate School of Engineering, Tohoku University, Aoba 6-6-01, Aramaki, Aoba-ku, Sendai 980-8579, Japan

E-mail: yanjw@pm.mech.tohoku.ac.jp (Jiwang Yan)

Received 12 January 2011, in final form 18 April 2011
Published 6 May 2011
Online at stacks.iop.org/JPhysD/44/215302

Abstract

In a glass moulding press (GMP) for refractive/diffractive hybrid lenses, to improve the service life of nickel–phosphorus (Ni–P) plated moulds, it is necessary to control the diffusion of constituent elements from the mould into the release agent coating. In this study, diffusion phenomena of constituents of Ni–P plating are investigated for two types of release agent coatings, iridium–platinum (Ir–Pt) and iridium–rhenium (Ir–Re), by cross-sectional observation, compositional analysis and stress measurements. The results show that Ni atoms in the plating layer flow from regions of compressive stress to regions of tensile stress. In the case of the Ir–Pt coated mould, the diffusion of Ni is promoted from the grain boundaries between the Ni and Ni_3P phases in the plating towards the surface of the Ir–Pt coating. However, in the Ir–Re coated mould, the diffusion of Ni is suppressed because the diffusion coefficient of Ni in the Ir–Re alloy is smaller than that in the Ir–Pt alloy, although the stress state is similar in both cases. By controlling the diffusion of Ni atoms, the use of Ir–Re alloy as a release agent coating for Ni–P plated moulds is expected to lead to a high degree of durability.

(Some figures in this article are in colour only in the electronic version)

1. Introduction

Optical and optoelectronic products such as digital cameras, mobile phones and high-density optical disc systems use many optical lenses. Generally, these lenses are made of plastic or glass. The advantage of plastic lenses is that they are cheaper. On the other hand, glass lenses have a high refractive index, high permeability to light and good stability against environmental changes. For this reason, recently, glass lenses are increasingly in demand in high-pixel-count digital cameras and in cameras used in mobile phones [1]. The demand for optical lenses in the car manufacturing industry may also increase in the future and such lenses need to be stable under changing temperature and humidity conditions. For most applications, such as digital cameras and mobile phones, the shape of the glass lenses is aspherical to improve the resolution and field angle and to reduce the size and weight of the optical system. The mass production technique for aspherical glass lenses is high-temperature glass moulding press (GMP), which has been already established [2].

Recently, Fresnel lenses and refractive/diffractive hybrid lenses of glass have been developed by introducing microgrooves onto aspherical surfaces. These kinds of lenses have much higher optical performance than aspherical lenses and enable miniaturization and cost reduction of digital optical products. For the purpose of mass production of glass Fresnel lenses and hybrid lenses, tungsten carbide moulds are currently used and the microgrooves on the moulds are generated by a microgrinding technique using sharply trued grinding wheels [3]. However, the sharp grinding wheels wear considerably,

which degrades mould form accuracy and raises production cost. To solve this problem, in a previous work, we developed a nickel–phosphorus (Ni–P)-plated mould with which such Fresnel lenses could be moulded [4]. Fine microstructures can be easily generated on the surface of the Ni–P plated mould using a single-crystal diamond cutting tool, and the moulds can be used to mould refractive/diffractive hybrid glass lenses and other microstructures at a temperature of 387 °C [4, 5]. However, in higher temperature moulding tests, we found that the constituent elements of the Ni–P plating diffuse into the release agent coating, resulting in mould surface roughening and adhesion of glass to the mould [6, 7].

To solve this problem, in this study, we investigated the diffusion phenomena of the constituents of the Ni–P plating at typical moulding temperatures for two types of release agent coatings. The change in internal stress of the Ni–P plating was also measured, and its relationship to the amount of atomic diffusion was examined. In addition, the influence of the type of release agent used on diffusion was evaluated.

2. Material interface design for GMP moulds

One crucial requirement of a mould for glass lenses is the demoulding ability. That is to say, the finished lens must be easily removed from the moulds. In high-temperature glass moulding, the surface of the mould tends to oxidize and the oxidized material diffuses into the glass, causing adhesion of the glass lens to the mould [8]. Therefore, a release agent is usually coated onto the surface of the mould to prevent oxidation. It is generally considered that the lifetime of a mould is almost completely determined by that of the release agent coating. Wearing and flaking of this coating reduces the lifetime of the mould. Moreover, deterioration of the oxidation resistance of the release agent due to in-diffusion of elements from the mould leads to an increased level of wettability by the glass which again reduces the mould lifetime. Thus, the lifetime of the mould is influenced both by interactions between the release agent and the mould and the release agent and the glass. Consequently, the choice of an appropriate release agent for the mould substrate is critical.

For tungsten carbide substrates that are most generally used as moulds for glass moulding, release agent coatings such as diamond-like carbon (DLC) [9], Ir–Pt alloy [10] and Ir–Re alloy [11] are used. However, since very little research has been carried out on the use of a mould comprising a Ni–P-plated substrate for the production of glass lenses, the most suitable release agent material is unknown at present. In our previous work [7], we found that when a combination of a Ni–P-plated substrate and an Ir–Pt coating were heated above 500 °C, Ni from the mould diffused into the Ir–Pt coating, which resulted in adhesion of the glass to the mould. Therefore, the choice of the release agent composition should be carefully considered in order to inhibit such diffusion and extend the mould lifetime above 500 °C.

Possible approaches to this problem are to reduce either the solubility limit of Ni or its diffusion coefficient in the release agent coating. However, it is easy for Ni to form intermetallic compounds with elements in which it has a low solubility limit; such compounds tend to have a completely different crystal structure from Ni and are weak [12]. This can lead to poor adhesion of the release agent to the Ni–P mould, causing it to flake off. Thus, it is preferable for Ni to have a high solubility limit in the release agent. On the other hand, release agents that have a low diffusion coefficient for Ni can both suppress Ni diffusion and provide good adhesion to the Ni–P substrate. Because the diffusion coefficient is correlated with the melting point for metals, elements that have a high melting point and a high Ni solubility limit might be most appropriate as release agents. Considering also the need for oxidation resistance, a list of candidate elements is shown in table 1. In this work, Re was chosen as one of the constituent elements because of its high melting point. In addition, since Ir and Ni are miscible in all proportions, Ir is expected to exhibit a high degree of adhesion to the Ni–P substrate. Therefore, an Ir–Re alloy was chosen as one of the release agent coatings in this study, and the results were compared with those for Ir–Pt. Although DLC also has a high melting point, it is likely that its adhesion to Ni–P would be poor, based on the non-solubility of Ni in this material. The applicability of DLC as a release agent coating for Ni–P is a subject for future study.

Table 1. Melting points and Ni solubility limits of candidate elements for release agent coating [17].

Elements	Melting point (°C)	Ni solubility limit (at%)
Pt	1769	100
Ir	2447	100
Re	3186	16.8
Os	3033	64.2
Ru	2334	50.3
C	3827	0

3. Experimental procedures

3.1. Mould fabrication

A cylindrical hot-work tool steel with a diameter of 18 mm and a thickness of 14 mm was used for mould substrates. After hardening, the substrates were electroless-plated with Ni–10 wt%P. The thickness of the plated layer was 70 μm. Next, the plated surface was polished to a mirror finish of optical grade and the release agent coating was applied. In this study, Ir, Ir–40 wt%Pt and Ir–50 wt%Re, respectively, were used as release agent coatings. The films were deposited by radio frequency (RF) magnetron sputtering and had a thickness of 300 nm. To improve the adhesion of the release agent coating to the Ni–P plating, a 50 nm-thick Ni interlayer was inserted between them. Figure 1 shows a schematic diagram of the mould structure, where t indicates thickness.

3.2. Thermal gravimetric analysis of release agent coating elements

Thermal gravimetric analysis was used to evaluate the oxidation resistance of the release agent elements. This

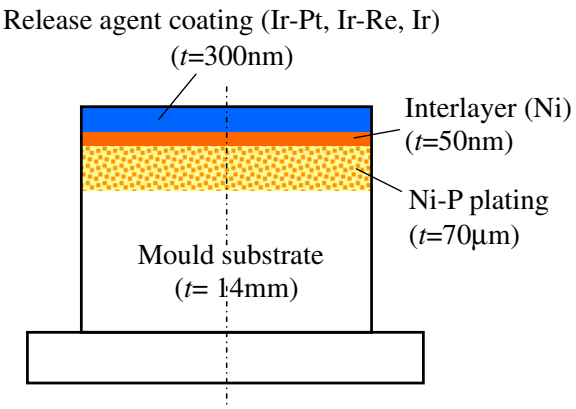

Figure 1. Schematic diagram of mould structure.

analysis was carried out on Ir–40 wt%Pt powder, Ir powder and Re wire. The Ir–40 wt%Pt powder was formed by grinding a sputtering target made by the solution process using a diamond grindstone. The Ir powder used had a purity of 99.999% and a maximum particle diameter of 150 μm. Because of the danger of ignition of Re in its powder form, a Re wire rod of 1 mm diameter was used. All samples were heated from room temperature to 1000 °C at a rate of 10 °C min^{-1} using a thermal analysis system (TG/DTA320, SII Nanotechnology Inc.) in air or in nitrogen, and the weight change of each sample was measured.

3.3. Measurement of mould surface roughness

We previously clarified that interdiffusion of the elements of the release agent and the Ni–P plating could occur at the moulding temperature of a glass lens [7]. Such interdiffusion causes an increase in the mould surface roughness and makes it difficult to remove the lens following moulding. Therefore, changes in the surface roughness of the moulds at typical glass-moulding temperatures were measured, in the presence of three kinds of release agent coatings (Ir–40 wt%Pt, Ir–50 wt%Re and Ir). In this study, only the effect of heating on the surface roughness was considered. In actual use, the mould would be subjected to even more severe conditions due to the application of pressure (∼MPa level). The moulds were heated in nitrogen at atmospheric pressure at 570 °C for 1–8 h, and the surface roughness was measured with a white-light interferometer (NewView 5022, Zygo Corp.) at a lateral resolution of 1 μm.

3.4. Observation on Ni–P plating microstructure

Microstructural changes in the Ni–P plating layer due to heating were investigated for two different release agent coatings (Ir–40 wt%Pt and Ir–50 wt%Re). Before deposition of the release agent coating, the composition profile of the plating layer was determined using x-ray diffraction (XRD; RINT1500, Rigaku Corp.) in combination with wet etching. The XRD measurements were carried out using Cu Kα x-rays. The wet etching was done using a 5% nital (ethanol +5% nitric acid) solution. The Ni phase was selectively etched by the nital solution, and the etched surface of the plating layer was observed by scanning electron microscopy (SEM;

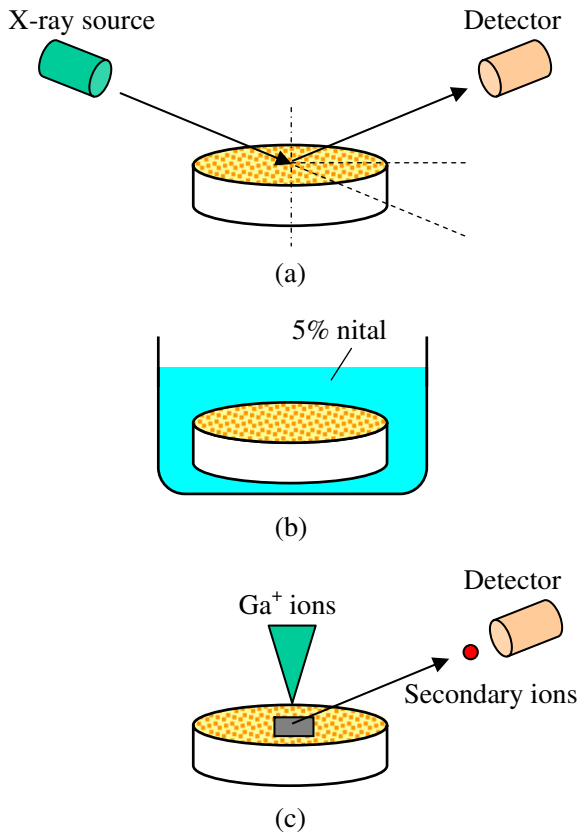

Figure 2. Microstructural observations of plating layer: (*a*) x-ray diffraction, (*b*) wet etching and surface SEM observation, (*c*) FIB processing and cross-sectional SIM observation.

S-3100, Hitachi Ltd.). Following the deposition of the release agent coating, cross sections of the samples were observed before and after heating using scanning ion microscopy (SIM; FB-2000A, Hitachi High-Technologies Corp.). The samples for SIM observations were prepared using focused ion beam milling (FIB; SMI3050MS2, SII NanoTechnology Inc.). A 5 μm × 5 μm region of the mould surface was etched by the ion beam to a depth of 3 μm for cross-sectional SIM observation. Figure 2 shows the schematic diagrams of the observation methods used.

3.5. Composition profile in release agent coating

The change in composition with depth from the mould surface was evaluated to determine the level of interdiffusion of elements between the release agent coating and the plating layer. The composition was analysed by secondary ion mass spectroscopy (SIMS; 6800T, PHI Co.) in a 125 μm × 250 μm region while etching with caesium (Cs^+) ions.

3.6. Stress measurement

The stress at the mould surface during thermal cycling was measured since such stress may influence atomic diffusion. To ease the stress measurement, thin square samples of mould substrates (30 mm × 30 mm × 1.5 mm) were prepared as test pieces. Ni–P plating and release agent layers were then deposited on the substrates to produce a cross-sectional

structure similar to that shown in figure 1. The warp (curvature radius) of the substrate was measured immediately after sputtering and during thermal cycling. In thermal cycling, the test piece was heated from room temperature to 600 °C and then naturally cooled down to room temperature again. The thermal cycle was performed in vacuum, and the rate of temperature change was 50 °C min^{-1} for both heating and cooling. The curvature can be either convex or concave depending on whether the thin film is under compressive or tensile stress, respectively. The curvature radius of the substrate was measured as shown in figure 3(*a*). Two parallel laser beams are irradiated on the substrate at the same time, and the reflected beams are captured by a CCD camera. When the substrate is warped, the spacing between the two reflected beams at the CCD camera changes by an amount δd relative to the original beam spacing d_0. The internal stress σ in the thin film is then given by Stoney's equation, as shown below as a function of the curvature radius R [13].

$$\sigma = \frac{E_s}{1-\nu_s}\frac{h_s^2}{12Lh_f}\left(\frac{\delta d}{d_0}\right)\cos\alpha = \frac{E_s h_s^2}{6(1-\nu_s)h_f}\frac{1}{R}. \qquad (1)$$

Here E_s is Young's modulus of the substrate, ν_s is the Poisson ratio of the substrate, R is the curvature radius of the test piece, L is the distance between laser beam A and the CCD measuring plane, h_s is the thickness of the substrate and h_f is the thickness of the thin film.

The curvature is defined as being positive when the plating layer side becomes concave, and negative when it becomes convex, as shown in figure 3(*b*). For instance, the curvature becomes positive if the plating layer is under tensile stress due to a decrease in the volume (shrinkage) of the plating layer. All measurement results are corrected by subtracting the original substrate curvature before deposition of the plating and release agent layers. Figure 3(*c*) shows the flow chart for producing the test pieces and carrying out the measurements.

3.7. Constituent concentration distribution analysis

In order to characterize the constituent concentration of the mould surface, the Ni–P-plated mould was first heated to a high temperature (920 °C). After heating, the mould surface was polished, and Ni interlayer and Ir–Pt layer were sputtered onto the mould surface. Then, the sputtered mould was heated again at a temperature of 570 °C for 1 h. The constituent concentration distribution of the mould surface before and after the second heating (at 570 °C) was analysed by an electron probe microanalyser (EPMA1610, Shimadzu Corp.), which has submicrometre level lateral resolution and vertical resolution of a few nanometres.

4. Results and discussion

4.1. Thermal gravimetric analysis results

Figures 4(*a*) and (*b*) show the weight changes for Ir–Pt alloy powder, Ir powder and Re wire during heating in air, and figure 4(*c*) shows results for heating in nitrogen, respectively. For Ir–Pt alloy and Ir, a similar trend is observed. In air, the

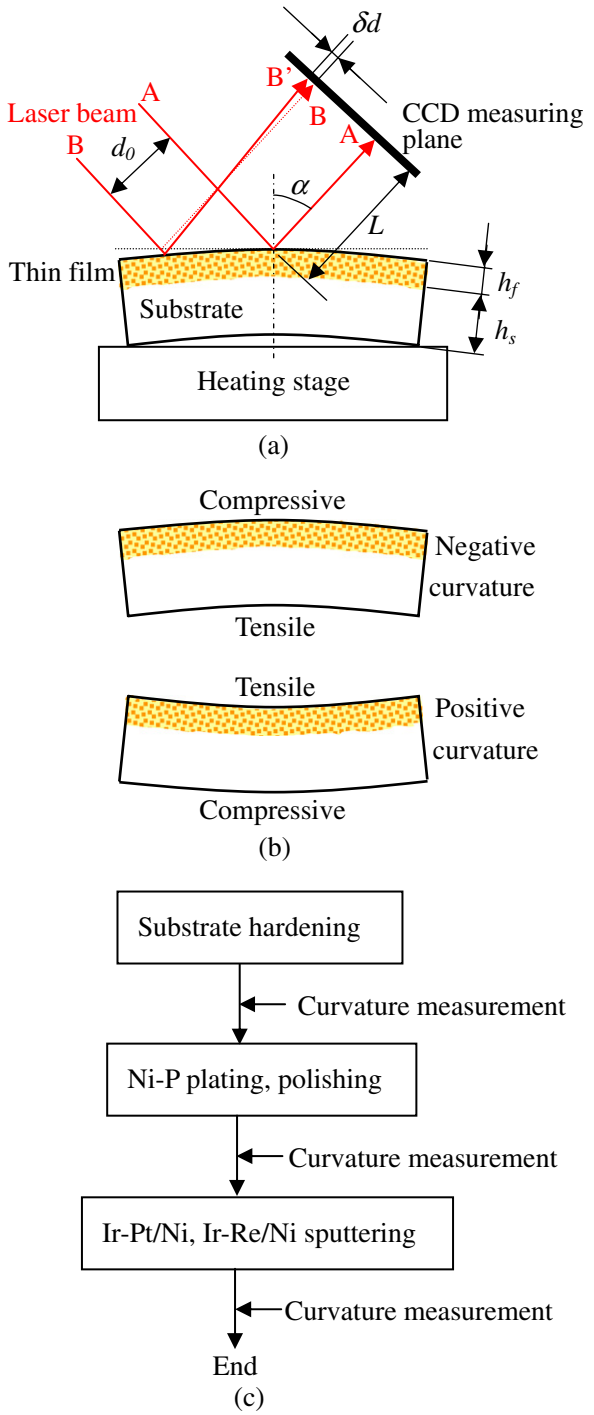

Figure 3. Method of stress measurement: (*a*) principle of warp measurement, (*b*) relation between specimen curvature and stress, (*c*) flow chart of stress measurement.

weight first begins to gradually increase with temperature, then more rapidly in the range 600–700 °C, before finally sharply decreasing at about 980 °C. In nitrogen, the weight gradually increases with temperature but no decrease is observed around 980 °C. The results in air can be explained by the formation of various oxides of Ir, such as IrO_2 (solid), Ir_2O_3 (gas) and IrO_3 (gas) as reported in previous work [14]. The initial increase in weight is thought to be due to the formation of IrO_2, which forms more quickly at 600–700 °C. At around 980 °C, Ir_2O_3 and IrO_3 start to be formed by oxidation of either Ir or IrO_2.

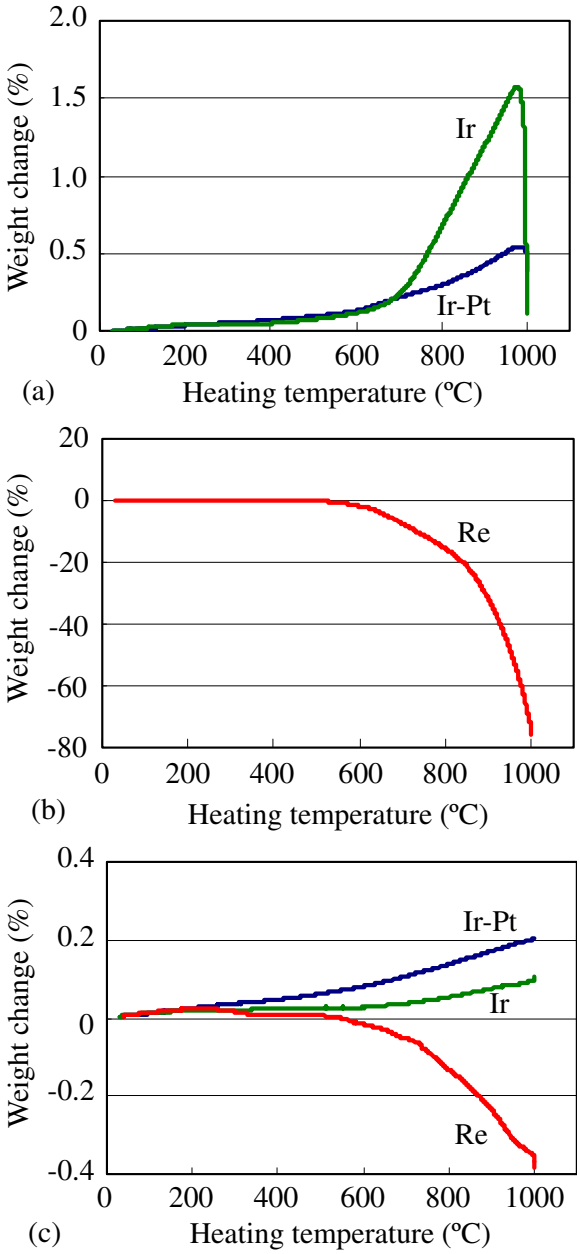

Figure 4. Weight change in the release agent coating materials: (*a*) Ir–Pt powder and Ir powder, and (*b*) Re wire during heating in air; (*c*) results for heating in nitrogen.

Since these are volatile compounds, their formation leads to a sharp decrease in weight. Heating in nitrogen does not seem to produce any significant amounts of Ir_2O_3 or IrO_3 since no weight decrease occurs. However, the slow increase in weight seems to indicate that IrO_2 is formed in a small quantity, probably due to residual oxygen in the nitrogen stream.

For the case of Re in air, a decrease in weight begins to occur at 500–600 °C and accelerates at 800 °C. All samples completely disappear by 1000 °C. In the nitrogen atmosphere, although a similar weight decrease begins at 500–600 °C, the rate of decrease is about 200 times less than that in air. The reported oxides of Re are Re_2O_3, ReO_2, Re_2O_5, ReO_3 and Re_2O_7 [15, 16]. The thermal stability of Re_2O_7 is low, sublimation begins at 250 °C, and it boils at 362 °C. Therefore, the weight decrease seems to be caused by the evaporation of

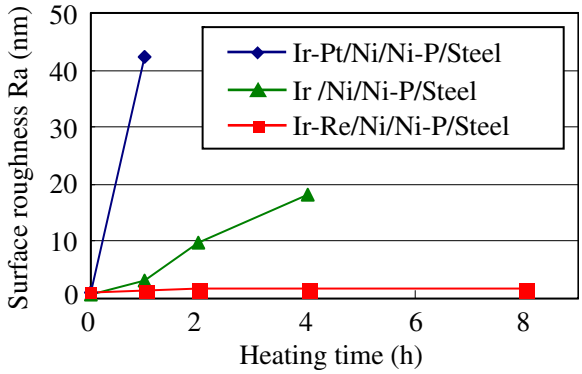

Figure 5. Relation between heating time and surface roughness of the mould.

Re_2O_7. The compound Re_2O_7 can be formed by either of the following reactions [15]:

$$3ReO_3 \leftrightarrow Re_2O_7 + ReO_2 \quad \text{(over 400 °C)} \qquad \text{(Reaction1)}$$

$$7ReO_2 \leftrightarrow 2Re_2O_7 + 3Re \quad \text{(700–800 °C)}. \qquad \text{(Reaction2)}$$

It is believed that the formed Re_2O_7 first begins to evaporate at 500–600 °C (Reaction 1), and undergoes accelerated evaporation at about 800 °C (Reaction 2). Although very little weight decrease occurs in nitrogen atmosphere, it appears that small quantities of Re_2O_7 can still be formed and evaporate above 600 °C.

In the temperature range 500–600 °C, which is typical for moulding glass lenses, Ir–Pt, Ir and Re all exhibit excellent oxidation resistance, and are suitable as release agent coatings. Moreover, because the rate of oxidation is influenced by the atmosphere present, it is thought that control of the atmosphere during the moulding process is important. In actual industrial applications, inert gases, such as nitrogen, are usually used as the moulding atmosphere.

4.2. Heating-induced change in the mould surface roughness

The relation between the heating time at 570 °C and the mould surface roughness is shown in figure 5 for Ir–40 wt%Pt, Ir–50 wt%Re and Ir release agents. In the case of Ir–Pt-coated mould, the roughness increases rapidly with heating time. In contrast, in the case of Ir–Re-coated mould, the surface roughness shows almost no dependence on heating time. In the Ir–Pt-coated mould, it is thought that Ni diffuses from the Ni–P layer and the interlayer into the release agent layer and the mould surface swells locally due to non-uniform diffusion rates [7], thus leading to an increase in the surface roughness. If this is the case, it appears that such diffusion is suppressed in the case of the Ir–Re-coated mould. A heating time of 8 h corresponds to 480 moulding operations, assuming a pressing time of 60 s in actual lens moulding. In the Ir-coated mould, the surface roughness increases with heating time, although in a more gradual manner than for the Ir–Pt-coated mould. The melting points of Ir–40 wt%Pt and Ir–50 wt%Re are about 1920 °C [17] and about 2800 °C [18], respectively, corresponding to the liquid phase generation temperatures from the binary phase diagrams. The melting point of Ir is 2447 °C [17]. Thus, the melting points increase

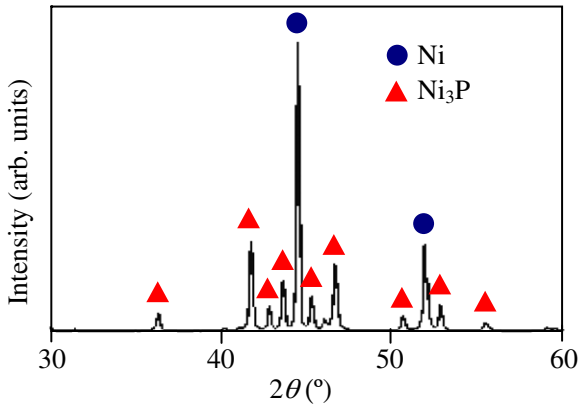

Figure 6. XRD spectrum from heated plating layer.

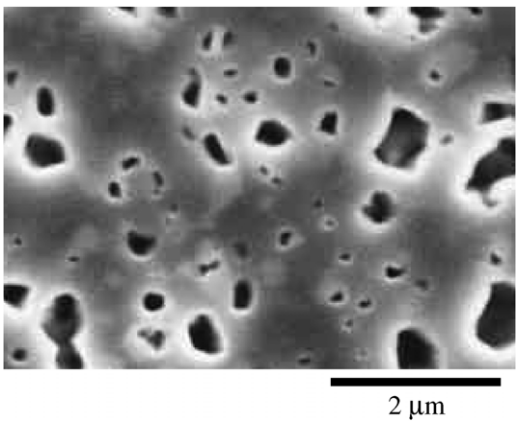

Figure 7. SEM image of heated plating layer after 5% nital etching.

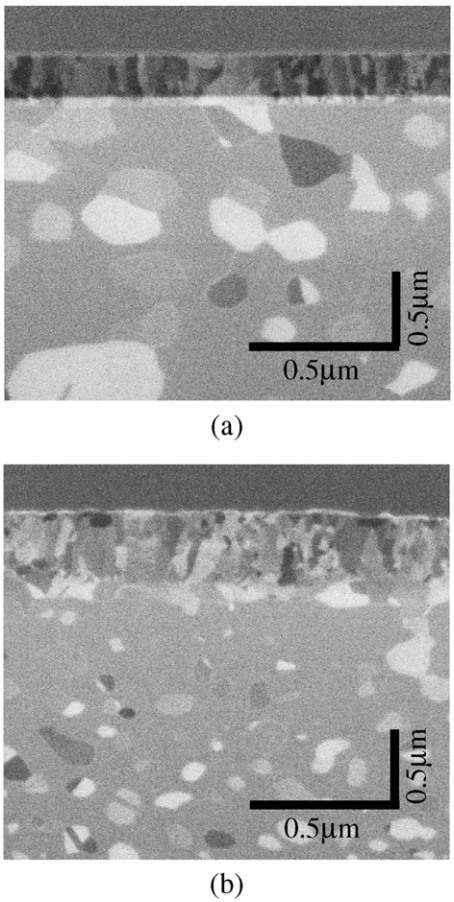

Figure 8. Cross-sectional SIM images of surface region of Ir–Pt-coated mould: (*a*) before heating, (*b*) after heating.

in the order Ir–40 wt%Pt, Ir and Ir–50 wt%Re. It is thought that the differences seen in figure 5 are influenced by the melting point of the release agent coating because there is a correlation between the melting point and the diffusion coefficient.

4.3. Structure of heated plating layer

Figure 6 shows the results of an XRD analysis of the plating layer following heating at 570 °C. The plating layer is composed of Ni and Ni_3P. Moreover, a surface SEM image of the plating layer after etching the Ni phases with 5% nital is shown in figure 7. The presence of submicrometre-sized voids indicates that, following heating, the plating layer has a microstructure comprising isolated regions of Ni in a Ni_3P matrix.

4.4. Cross-sectional observation of the release agent coating

Figures 8 and 9 show the cross-sectional SIM images of the Ir–Pt-coated and Ir–Re-coated moulds, respectively, before and after heating at 570 °C for 1 h. Ni crystals can be clearly seen in the Ni_3P matrix in the plating layer; the variations in the shading of these crystalline regions are due to the presence of different crystallographic orientations. For the Ir–Pt-coated mould, the interlayer disappears after heating. In addition, the thickness of the release agent coating increases to about 700 nm from about 300 nm before heating. Moreover, the density of the Ni phase regions near the release agent coating decreases, and the average size of these regions decreases throughout the Ni–P layer. For Ni–P-plated moulds coated with Ir–Pt, the Ni element in the plating layer diffuses into the Ir–Pt coating [7]. The consumption of Ni appears to begin in the neighbourhood of the Ir–Pt coating, but it is thought that Ni later diffuses even from the deeper regions towards the interface with the Ir–Pt layer. In the case of the Ir–Re-coated mould, on the other hand, the appearance of the plating layer and release agent coating does not change remarkably following heating.

4.5. Changes in the near-surface compositions

We have previously reported that when the Ir–Pt-coated mould is heated at 570 °C for 1 h, the Ni and P in the plating layer diffuse into the release agent coating and Ir and Pt in the release agent coating diffuse into the plating layer [7]. After heating, a remarkable amount of Ni diffusion occurs into the Ir–Pt coating until the Ni concentration gradient between the Ir–Pt coating and the plating layer almost disappears, though Ni did not exist in the Ir–Pt coating before heating. Figure 10 shows the results of a SIMS analysis of the Ir–Re-coated mould before and after heating. The horizontal axis represents the depth from the surface and the vertical axis the number of secondary ions generated by the caesium ion irradiation; this number corresponds to the concentration of each element. No major

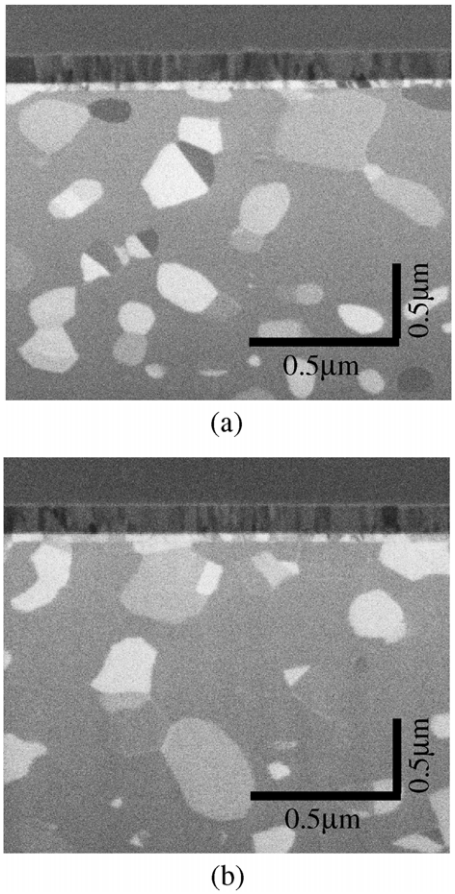

Figure 9. Cross-sectional SIM images of surface region of Ir–Re-coated mould: (*a*) before heating, (*b*) after heating.

changes are seen in the distribution of each element following heating, apart from some diffusion of P into the Ni interlayer.

4.6. Stress in Ni–P plating layer

The change in the curvature (warp) during heating and cooling is shown in figure 11(*a*) for a bare steel substrate and in figure 11(*b*) for a substrate with a 70 μm-thick Ni–P plating layer. Figure 12(*a*) replots the data shown in figure 11(*b*) after correcting it for the curvature of the steel substrate itself shown in figure 11(*a*); this thus represents the curvature due to the Ni–P layer alone.

As shown in figure 12(*a*), the changes in curvature are found to be different between the first and second thermal cycles. The plating layer is initially amorphous but becomes polycrystalline during the first thermal cycle. It is thought that this transformation is the reason for the drastic change in the curvature at about 480 °C [19] during the first cycle. Following the second thermal cycle, the changes in the curvature became steady and repetitive. The internal stress calculated from figure 12(*a*) using Stoney's equation is shown in figure 12(*b*). This represents the mean stress acting on the plating layer, with positive values corresponding to tensile stress and negative values to compressive stress. Following crystallization of the plating layer, a tensile stress of about 250 MPa is present at room temperature, and this decreases to about 50 MPa by heating up to 600 °C. Since no further transformations

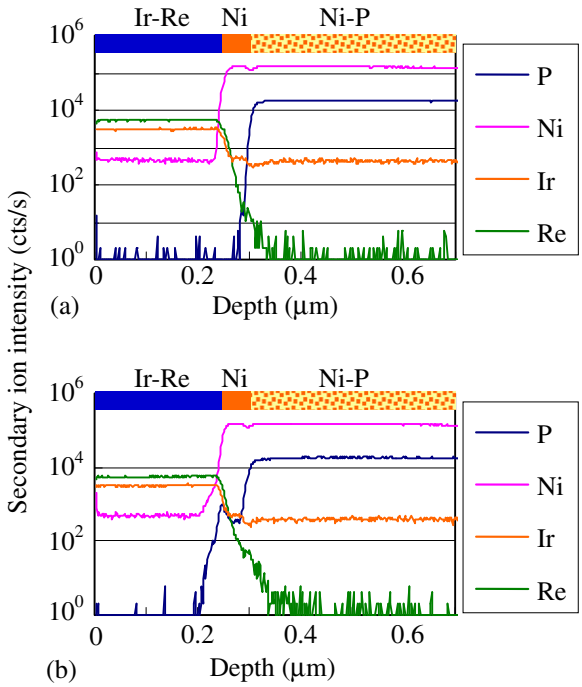

Figure 10. Depth distribution of elements in Ir–Re-coated mould: (*a*) before heating, (*b*) after heating at 570 °C for 1 h.

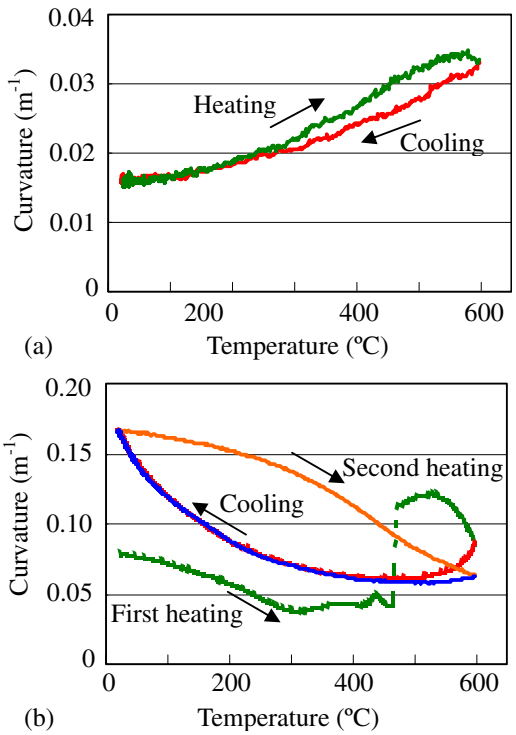

Figure 11. Curvature changes of (*a*) steel substrate and (*b*) Ni–P/steel substrate during heating and cooling.

occur, this stress is thought to be due to differences in the thermal expansion coefficients of the plating layer and the steel substrate. The fact that the tensile stress decreases as a result of heating, and increases as a result of cooling, indicates that the thermal expansion coefficient of the plating layer is larger than that of the steel substrate.

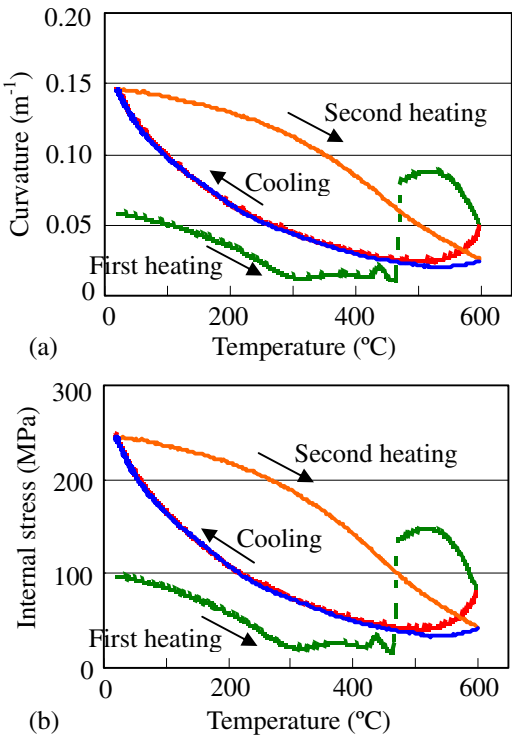

Figure 12. (*a*) Curvature change and (*b*) internal stress of Ni–P plating layer during heating and cooling.

4.7. Stress in Ni–P layer after release agent coating

Figures 13(*a*) and (*b*) show the stress curves during thermal cycling for the Ir–Pt-coated and Ir–Re-coated moulds, respectively. The second-cycle curve for the Ni–P only case is shown for comparison in both figures. It can be seen that there are no major differences between the curves for the Ir–Pt-coated and Ir–Re-coated moulds. In both cases, there is an increase in the room-temperature tensile stress before thermal cycling compared with the Ni–P only case. It is thought that this stress is due both to lattice mismatch between the plating and sputtered layers, and the unstable atomic arrangement due to the inability of surface atoms to diffuse at this temperature [20]. This additional tensile stress component disappears during the first thermal cycle and the stress curves subsequently retrace each other. This is thought to be due to plastic deformation of the Ni interlayer to accommodate the stress.

In addition to the increased initial tensile stress at room temperature, both the Ir–Pt-coated and Ir–Re-coated moulds exhibit true compressive stress at higher temperatures. In the case of the Ni–P only mould, there was a tendency towards the compressive stress direction at high temperatures due to the Ni–P layer being constrained by the steel substrate with a smaller thermal expansion coefficient. However, the thermal expansion coefficient of the Ni–P plating is also higher than that of the Ni interlayer and the release agent coating [18, 21]. This means that the Ni–P plating is constrained on both sides by materials with lower thermal expansion coefficients and true compressive stress is produced at higher temperatures.

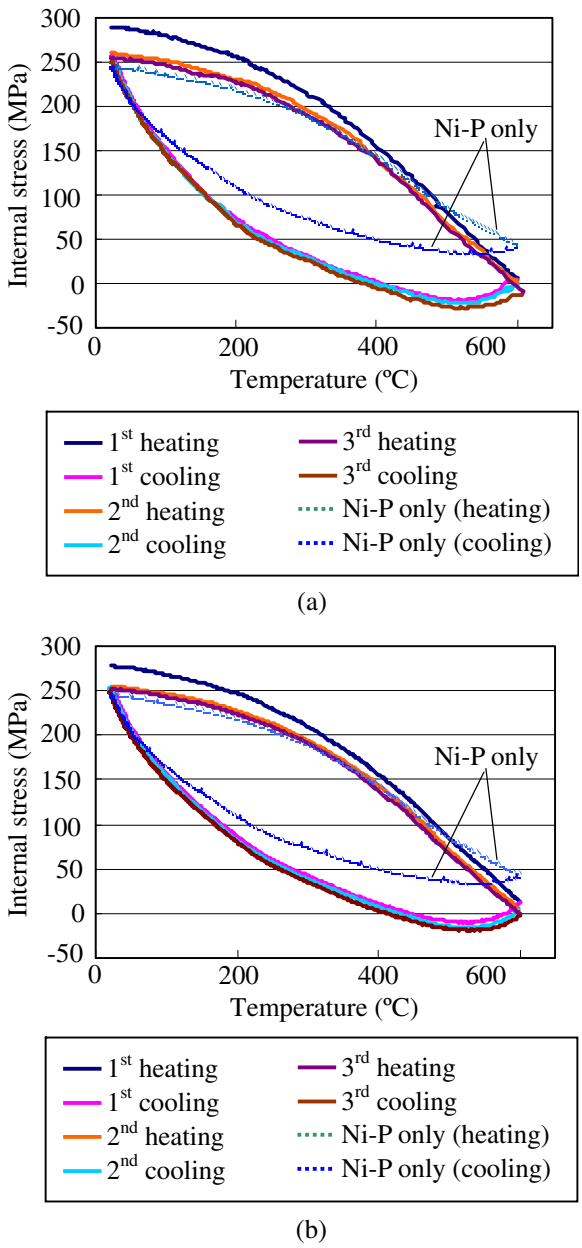

Figure 13. Internal stress change during heating and cooling at the surface of (*a*) Ir–Pt-coated mould (Ir–Pt/Ni/Ni–P) and (*b*) Ir–Re-coated mould (Ir–Re/Ni/Ni–P).

4.8. Diffusion mechanism of Ni atoms

In general, diffusion of atoms is influenced by the presence of stress. The relation between the atomic flux J_S (g cm^{-2} s^{-1}) and the stress gradient is given by [22, 23]

$$J_S = \frac{C\Omega}{k_B T} D_0 \exp\left(-\frac{Q - \Omega\sigma}{k_B T}\right) \operatorname{grad}\sigma. \qquad (2)$$

Here C is the atomic concentration, Ω is the atomic volume, k_B is Boltzmann's constant, T is the absolute temperature, D_0 is the self-diffusion coefficient, Q is the activation energy and σ is the hydrostatic stress. According to this expression, atoms flow from regions of higher compressive stress to regions of lower compressive stress, and the flux is proportional to the stress gradient.

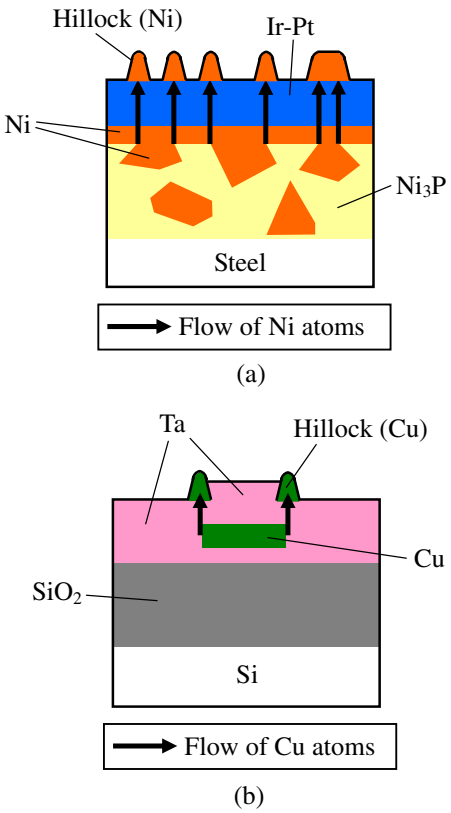

Figure 14. Atomic diffusion models: (*a*) diffusion of Ni in Ir–Pt-coated mould, (*b*) Settsu's model for diffusion of Cu in Ta.

Figure 14(*a*) shows a schematic of Ni diffusion in the Ir–Pt-coated mould. It is thought that during heating, a stress gradient is generated at the interface between the release agent coating and the plating layer due to the difference in the thermal expansion coefficients. As a result, Ni atoms diffuse from the Ni crystal boundaries towards the surface of the release agent coating, and swelling occurs at the surface. Settsu *et al* explained a similar phenomenon to this using the model shown in figure 14(*b*) [24]. It consists of a Cu film embedded in a Ta layer on a SiO_2/Si substrate. The thermal expansion coefficients of Ta and Cu are $6.6 \times 10^{-6}\,K^{-1}$ and $16.2 \times 10^{-6}\,K^{-1}$, respectively. When the sample is heated, Cu is subjected to compressive stress since it has a higher thermal expansion coefficient than Ta. The compressive stress distribution has minimum values at the corners of the rectangle. Thus, Cu atoms in regions of high compressive stress move to the corners of the Cu film, and the stress distribution in the Cu eventually becomes uniform. These Cu atoms are then driven towards the low-stress Ta surface under the influence of the stress gradient. They diffuse along grain boundaries in the Ta to form hillocks on the Ta surface.

This concept can also be applied to the case of Ni diffusion in the Ir–Pt-coated mould. The regions of Ni phase are distributed in the Ni_3P matrix in the plating layer as shown in figure 14(*a*). The thermal expansion coefficients of Ni_3P and Ni at 500 °C are $12.7 \times 10^{-6}\,K^{-1}$ and $15.2 \times 10^{-6}\,K^{-1}$, respectively [18, 25]. In the Ir–Pt-coated mould, the Ni in the plating layer corresponds to the Cu in the Settsu model. During heating, the Ni atoms move to the corner regions of the Ni phases, and diffuse towards the surface of the Ir–Pt coating, resulting in the formation of hillocks (Ni) on the surface. It should be noted that the Ni in the interlayer also diffuses towards the release agent coating. However, since the interlayer is under tensile stress, the diffusion from the interlayer should be inactive compared with that from the Ni–P plating layer. In addition, the thickness of the interlayer (50 nm) is distinctly smaller than that of the plating layer (70 μm), thus, the amount of diffusion from the interlayer will be far smaller than that from the plating layer.

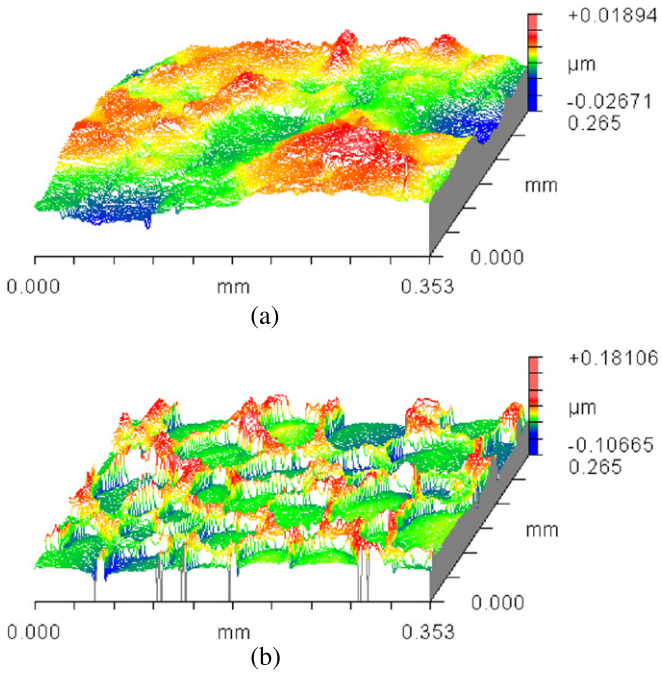

Figure 15. Surface topography of Ir–Pt-coated mould with large Ni–P crystal grains scanned with a white light interferometer: (*a*) before heating, (*b*) after heating at 570 °C for 1 h [7].

Figure 15 shows surface topographies of the Ir–Pt-coated mould with large Ni–P crystal grains before and after heating for 1 h at 570 °C. The topography was obtained by scanning with a white light interferometer. Following heating, the Ir–Pt coating swells in the region of the grain boundaries between the Ni and Ni_3P phases in the underlying plating layer [7]. However, when a Ni–P-plated mould without a release agent coating is heated at 570 °C, no change occurs in the surface roughness [7]. This is also consistent with the Settsu model.

The surface of the same sample as in figure 15 was analysed with EPMA. The constituent concentration distributions of the Ir–Pt-coated mould before and after heating are shown in figures 16 and 17, respectively. The colour bar is characteristic x-ray intensity, and corresponds to the relative concentration of each element. It is noteworthy that Ni was detected from the sample surface before heating, as shown in figure 16(*d*). This might be the response from the Ni element in the deeper region, i.e. the interlayer or the plating layer, as the penetration depth of the electron beam into a material is usually in the submicrometre level. However, after heating, the segregation of Ni in the hillocks was clearly confirmed on the surface of the Ir–Pt-coated mould, as shown in figures 17(*d*), demonstrating the atomic diffusion of Ni to the surface.

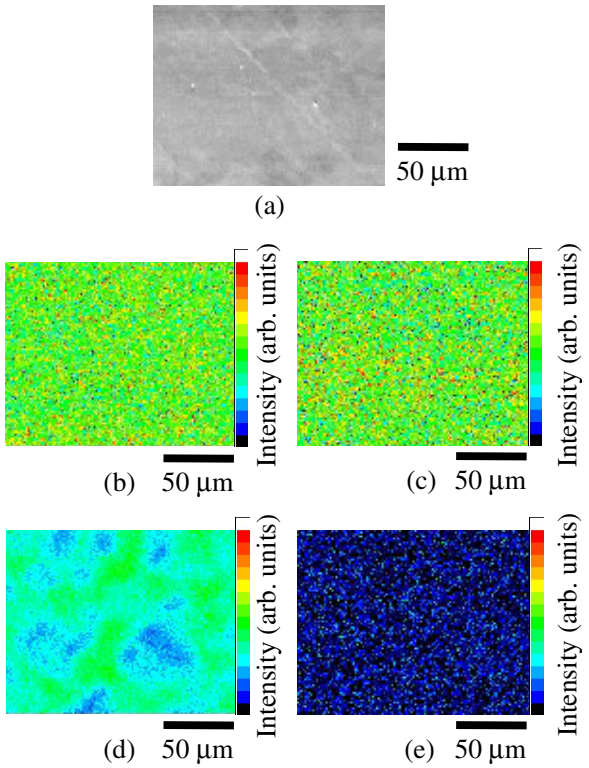

Figure 16. (*a*) SEM image, and EPMA mapping of Ir–Pt-coated mould surface before heating: (*b*) Ir, (*c*) Pt, (*d*) Ni, (*e*) P.

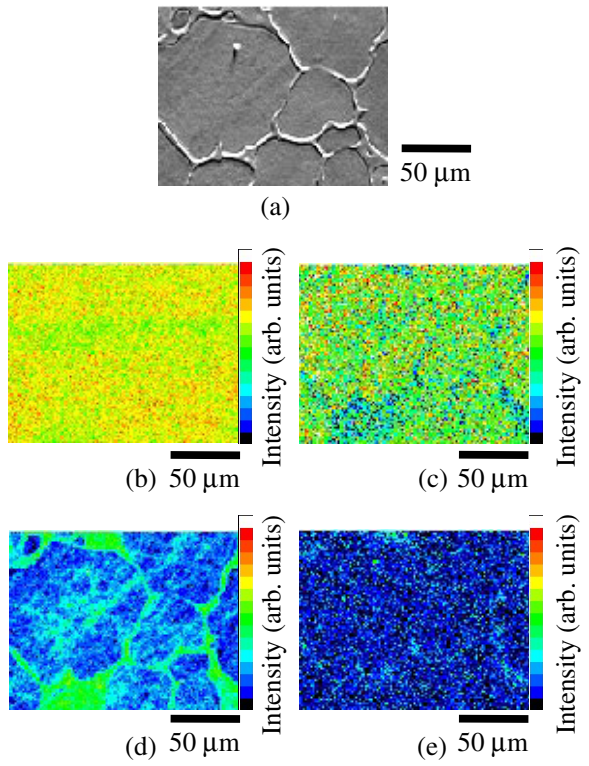

Figure 17. (*a*) SEM image, and EPMA mapping of Ir–Pt-coated mould surface after heating: (*b*) Ir, (*c*) Pt, (*d*) Ni, (*e*) P.

4.9. Diffusion controlling effect of Ir–Re coating

Comparing figures 13(*a*) and (*b*), it is evident that almost equal stress acted on the Ir–Pt-coated and Ir–Re-coated moulds. However, in the Ir–Re-coated mould, the diffusion of Ni from the plating layer into the release agent layer is suppressed. The reason for this may be as follows.

The diffusion coefficient D is given by the following equation in an area where a stress has been generated [26]:

$$D = D_0 \exp\left(-\frac{Q}{k_B T}\right) \exp\left(-\frac{\sigma V_a}{k_B T}\right). \tag{3}$$

Here D_0 is the frequency factor, Q is the activation energy, k_B is Boltzmann's constant, V_a is a constant known as the activation volume and represents the volume of the lattice directly affected by the diffusing atom, T is the absolute temperature and σ is the stress. Thus, D is the product of a term that depends on the activation energy and a term that depends on the stress. It is thought that the difference in the diffusion behaviour in the Ir–Pt-coated and Ir–Re-coated moulds is mainly related to the difference in activation energy because the stress is almost the same in both cases.

Here, we consider the diffusion coefficient ratio ($D_{\text{Ir–Pt}}/D_{\text{Ir–Re}}$) for the Ir–Pt-coated and Ir–Re-coated moulds. The stress-dependent term in equation (3) is considered to be the same for the Ir–Pt-coated and Ir–Re-coated moulds, based on the results shown in figures 13(*a*) and (*b*). Moreover, the frequency factor D_0 can be disregarded because it has no temperature dependence. Therefore, $D_{\text{Ir–Pt}}/D_{\text{Ir–Re}}$ can be expressed by

$$\frac{D_{\text{Ir–Pt}}}{D_{\text{Ir–Re}}} = \exp\left(\frac{Q_{\text{Ir–Re}} - Q_{\text{Ir–Pt}}}{k_B T}\right). \tag{4}$$

The activation energy Q for grain boundary diffusion in metal is approximated by $Q = 10 k_B T_m$, and depends on the melting point T_m of the diffusion medium [27]. The melting points of Ir–40 wt%Pt and Ir–50 wt%Re are assumed to be $T_{m(\text{Ir–Pt})} = 2193$ K and $T_{m(\text{Ir–Re})} = 3073$ K, respectively, which correspond to the liquid phase generation temperature from the binary phase diagram [17, 18]. Then, equation (4) can be simplified as

$$\frac{D_{\text{Ir–Pt}}}{D_{\text{Ir–Re}}} = \exp\left(\frac{10(T_{m(\text{Ir–Re})} - T_{m(\text{Ir–Pt})})}{T}\right) = \exp\left(\frac{8800}{T}\right). \tag{5}$$

The temperature dependence of the diffusion coefficient ratio ($D_{\text{Ir–Pt}}/D_{\text{Ir–Re}}$) is then plotted in figure 18. $D_{\text{Ir–Pt}}/D_{\text{Ir–Re}}$ has a value of $4.8 \times 10^5 \sim 2.4 \times 10^4$ at 400–600 °C that corresponds to the moulding temperature of a glass lens. Because the atomic diffusion length is proportional to the square root of the diffusion coefficient, the ratio of the diffusion lengths for the Ir–Pt-coated and Ir–Re-coated mould is in the range 700–150. Thus, it is thought that the Ir–Re-coated mould can suppress Ni diffusion because the diffusion coefficient in the release agent coating at the typical moulding temperature of glass lenses is smaller than that in the Ir–Pt-coated mould.

5. Conclusions

Ni–P-plated moulds with different release agent coatings were heated, and the diffusion of Ni was investigated

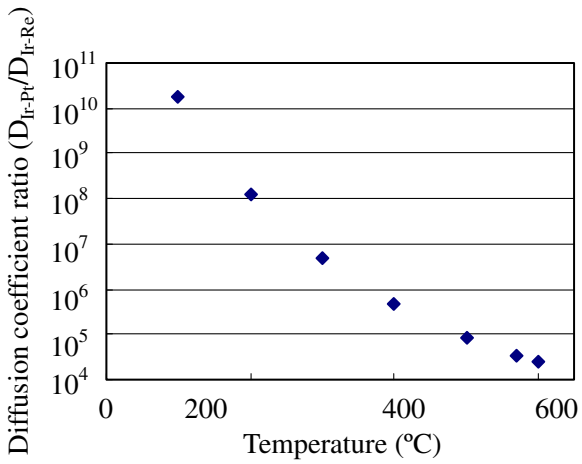

Figure 18. Diffusion coefficient ratio ($D_{Ir–Pt}/D_{Ir–Re}$) of the Ir–Pt-coated and the Ir–Re-coated moulds.

by cross-sectional observation, compositional analysis and stress measurements. The following conclusions were drawn.

(1) In the Ir–Pt-coated mould, Ni in the Ni–P plating layer and the interlayer diffuses towards the Ir–Pt coating during heating, and the mould surface becomes rough due to the accumulation of Ni. On the other hand, Ni diffusion is suppressed in the Ir–Re-coated mould during a similar heat treatment, and no change in the surface roughness occurs.

(2) When the moulds are subjected to thermal cycling, thermal stress is generated by the interfaces of the Ni–P plating layer, the steel substrate and the release agent coating. Since the thermal expansion coefficient of the plating is larger than that of the mould substrate and overlying sputtered layers, the internal stress in the plating layer becomes compressive at higher temperatures.

(3) The Ni atoms in the plating layer flow from regions of compressive stress to regions of tensile stress. In the case of the Ir–Pt-coated mould, the diffusion of Ni is promoted from the grain boundaries between the Ni and Ni_3P phases in the plating structure towards the surface of the Ir–Pt coating. However, in the Ir–Re-coated mould, the diffusion of Ni is suppressed because the diffusion coefficient of Ni in the Ir–Re alloy is smaller than that in the Ir–Pt alloy, although the stress is similar in both cases.

(4) By controlling the diffusion of Ni atoms, the use of Ir–Re alloy as a release agent coating for Ni–P-plated moulds is expected to lead to a high degree of durability.

Acknowledgment

This work is supported by the Japan Society for the Promotion of Science, Grant-in-Aid for Scientific Research (B), project number 19360055.

References

[1] Kinoshita H 2006 Optical lens *Ceram. Japan* **41** 872–3
[2] Yan J, Zhou T, Yoshihara N and Kuriyagawa T 2009 Shape transferability and microscopic deformation of molding dies in aspherical glass lens molding press *J. Manuf. Technol. Res.* **1** 85–102
[3] Suzuki H, Kamano T, Higuchi T, Tanioka T, Shimamura K, Yokoyama M, Kitajima T and Okuyama S 2001 Precision glass molding of micro Fresnel lens—experimental study on molding characteristics with molding conditions and feasibility study *J. Japan Soc. Precision Eng.* **67** 438–43
[4] Masuda J, Yan J and Kuriyagawa T 2007 Application of the NiP-plated steel molds to glass lens molding *Proc. 10th Int. Symp. on Advances in Abrasive Technology (ISAAT2007) (Dearborn, MI, 25–28 September 2007)* pp 123–30
[5] Yan J, Oowada T, Zhou T and Kuriyagawa T 2009 Precision machining of microstructures on electroless-plated NiP surface for molding glass components *J. Mater. Process. Technol.* **209** 4802–8
[6] Zhou T, Yan J, Masuda J, Oowada T and Kuriyagawa T 2011 Investigation on shape transferability in ultraprecision glass molding press for microgrooves *Precision Eng.* **35** 214–20
[7] Masuda J, Yan J, Tashiro T, Fukase Y, Zhou T and Kuriyagawa T 2009 Microstructural and topographical changes of Ni–P plated moulds in glass lens pressing *Int. J. Surf. Sci. Eng.* **3** 86–102
[8] Adams R B and Pask J A 1961 Fundamentals of glass-to-metal bonding: VII. Wettability of iron by molten sodium silicate containing iron oxide *J. Am. Ceram. Soc.* **44** 430–3
[9] Kim H U, Jeong S H, Kim H J and Kim J H 2007 Optical properties of aspheric glass lens using DLC coating mold *Key Eng. Mater.* **345–346** 1577–80
[10] Kuribayashi K, Monji H, Sakai M, Aoki M and Umetani M 1989 Sputter-deposited platinum alloy films for molding dies *J. Surf. Finish. Soc. Japan* **40** 907–11
[11] Kim S S, Kim H U, Kim H J and Kim J H 2007 Re–Ir coating effect of molding core (WC) surface for aspheric glass lens *Proc. SPIE* **6717** 671708
[12] Sudo H, Tamura I and Nishizawa T 1972 *Metallography* (Tokyo: Maruzen Publications)
[13] Hoffman R W 1966 *Physics of Thin Films* ed G Hass and R E Thun (New York: Academic)
[14] Carpenter J H 1989 Equilibrium reaction of iridium and oxygen at high temperatures *J. Less-Common Met.* **152** 35–45
[15] Kubo R, Nagakura S, Iguchi H and Enaga H 1987 *Physics and Chemistry Dictionary* 4th edn (Tokyo: Iwanami Shoten Publications)
[16] Samsonov G V 1970 *The Oxide Handbook* (Tokyo: Japanese–Soviet News Agency)
[17] Alloy Phase Diagram and Handbook Committees 1992 *ASM Handbook* vol 3 *Alloy Phase Diagrams* (Metals Park, OH: ASM International)
[18] The Japan Institute of Metals 1993 *Metals Data Book* (Tokyo: Maruzen Publications)
[19] Masui K, Maruno S and Yamada T 1977 Heat-induced structural changes in electrodeposited Ni–P alloys *J. Japan Inst. Met.* **41** 1130–6
[20] Miura H 1995 Residual stress of thin films *J. Japan. Soc. Tribologists* **40** 228–33
[21] Lu K and Sui M L 1995 Thermal expansion behaviors in nanocrystalline materials with a wide grain size range *Acta Metall. Mater.* **43** 3325–32
[22] Herring C 1950 Diffusion viscosity of a polycrystalline solid *J. Appl. Phys.* **21** 437–45
[23] Korhonen M A, Børgesen P, Tu K N and Li C-Y 1993 Stress evolution due to electromigration in confined metal lines *J. Appl. Phys.* **73** 3790–9

[24] Settsu N, Saka M and Yamaya F 2008 Fabrication of Cu nanowires at predetermined positions by utilising stress migration *Strain* **44** 201–8

[25] Samsonov G V and Paderno Y B 1971 Physical properties of lower nickel phosphides *Powder Metall. Met. Ceram.* **10** 565–7

[26] Kao D B, McVittie J P, Nix W D and Saraswat K C 1988 Two-dimensional thermal-oxidation of silicon: II. Modeling stress effects in wet oxides *IEEE Trans. Electron Device* **35** 25–37

[27] Cottrell A H 1970 *An Introduction to Metallurgy* (Tokyo: AGNE Publications)